Production of ω mesons in proton-proton collisions

K. Nakayama,[1,2] A. Szczurek,[3] C. Hanhart,[1] J. Haidenbauer,[1] and J. Speth[1]
[1]*Institut für Kernphysik, Forschungszentrum Jülich GmbH, D-52425 Jülich, Germany*
[2]*Department of Physics and Astronomy, University of Georgia, Athens, Georgia 30602*
[3]*Institute of Nuclear Physics, PL-31-342 Cracow, Poland*
(Received 21 November 1997)

The production of ω mesons in proton-proton collisions for proton incident energies up to 2.2 GeV is investigated within a meson-exchange model of hadronic interactions. We find a large cancellation between the dominant $\pi\rho\omega$ meson-exchange current and nucleonic current contributions. A comparison with preliminary data from SATURNE calls for the inclusion of off-shell form factors at the $NN\omega$ and $\pi\rho\omega$ production vertices. Due to the present lack of knowledge of these form factors, together with the destructive interference mentioned above, the relative magnitude of the nucleonic and meson-exchange current contributions cannot be determined from existing total cross section data. However, it is shown that the angular distribution of the produced ω mesons provides a unique and clear signature of the magnitude of these currents, thus allowing one to disentangle these two basic reaction mechanisms. [S0556-2813(98)06204-9]

PACS number(s): 13.75.Cs, 13.60.Le, 25.40.−h

I. INTRODUCTION

Vector-meson production in both hadronic and electromagnetic processes is considered to be an excellent tool for investigating the properties of vector mesons, both in medium and in free space. The properties of these mesons in the nuclear medium appear to be of special interest not only for the understanding of the nuclear dynamics but also for possibly revealing information about the deconfinement phase transition of hadrons to the quark-gluon plasma or the restoration of chiral symmetry at high baryon density and/or temperature [1–4]. The investigation of vector meson production processes in free space is important too. In addition to providing the necessary elementary production amplitudes required for in-medium studies, one can address other basic questions. For example, the nucleon-nucleon-vector-meson (NNv) vertex functions, even on the mass shell (coupling constants), are largely unknown, especially for the ω and ϕ mesons. Vector-meson production in proton-proton (pp) collisions may offer a means of extracting these coupling constants. Specifically, in the case of the ϕ-meson production, one might be able to obtain information on the strangeness content of the nucleon.

Therefore it might be surprising that very little information about vector-meson production processes can be found in the literature. Only quite recently have these reactions begun to receive increasing attention. For example, the near-to-threshold production of ω mesons in the reaction $p+d \rightarrow {}^3\mathrm{He}+\omega$ has been investigated both experimentally [5] and theoretically [6,7]. Also the production of both the ω and ϕ mesons in pp collisions close to threshold is now being analyzed by the SPES3 Collaboration at SATURNE (Saclay) [8] and will soon be studied at COSY (Jülich) [9]. From the theoretical side, Sibirtsev [10] has investigated the ρ-, ω-, and ϕ meson production within a simple one-pion exchange model, utilizing parametrizations of the measured cross sections in $\pi N \rightarrow vN$ ($v=\rho,\omega,\phi$) processes. Chung *et al.* [11] have calculated the ϕ-meson production in π-baryon and baryon-baryon collisions within the meson-exchange picture.

Clearly these works aim mainly at a parametrization of the $N+N \rightarrow N+N+v$ reactions, which is suitable for application in investigations of vector-meson production in proton-nucleus and heavy-ion collisions [12–14], and not so much at a detailed analysis of these reactions themselves. In particular, in none of these calculations is the NN final-state interaction (FSI) taken into account. In particle production reactions near their kinematical thresholds the final NN subsystem emerges at fairly low energies. Therefore, the nucleons are mainly in s-wave states where their interaction is very strong. Indeed, large effects of the NN FSI are well known from other processes such as the $N+N \rightarrow N+N+\gamma$ [15] and $N+N \rightarrow N+N+\pi$ reactions [16].

In the present work we focus on the $p+p \rightarrow p+p+\omega$ process. The reason for studying ω-meson production is that, in contrast to other vector-meson production reactions, only a few relevant basic production mechanisms are involved, and consequently, it is the simplest reaction among the various vector-meson productions in pp collisions. We describe this reaction within a meson-exchange model which takes the NN FSI into account. Our model calculation includes both the nucleonic and meson-exchange currents as defined below. The initial state interaction (ISI) is neglected. In this regard we mention that, quite recently, Batinić *et al.* [17] has examined its influence for the case of the reaction $p+p \rightarrow p+p+\eta$. These authors found that the ISI leads only to an overall reduction of the total cross section (by about 40%) but has virtually no effect on its energy dependence. Based on this result we would not expect any significant influence of the ISI on the qualitative aspects of ω production discussed in the present work.

The paper is structured as follows: In Sec. II we describe the details of our model. We give the basic formalism and specify the parameters entering into the numerical computations. The results of our calculations are presented in Sec. III where we show that the nucleonic current as well as the $\pi\rho\omega$ meson-exchange current yield potentially large contributions to the ω-production cross section. The inclusion of form factors at the ω-production vertices is necessary if one wants to

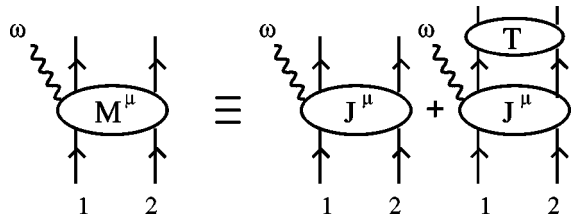

FIG. 1. The transition amplitude for the reaction $p+p\rightarrow p+p+\omega$.

achieve results comparable (in magnitude) to the preliminary data from SATURNE. We also find a strong cancellation between the contributions from the nucleonic current and meson-exchange currents—which makes it rather difficult to discriminate between these two production mechanisms from a study of the total cross section alone. Fortunately, as we shall demonstrate, the angular distribution of the produced ω mesons shows a clear dependence on the magnitude of these currents and is therefore suitable for disentangling the two dominant reaction mechanisms in question. A summary of our results is given in Sec. IV.

II. DETAILS OF THE MODEL

We write the transition amplitude describing the $p+p\rightarrow p+p+\omega$ process as

$$M^{\mu}=\langle\phi_f|(T_f^{(-)\dagger}G_f+1)J^{\mu}|\phi_i\rangle \ , \tag{1}$$

where $\phi_{i,f}$ denotes the four-component unperturbed NN wave function in the initial (i) and final (f) state. $T_f^{(-)}$ is the final state NN T matrix. G_f stands for the two-nucleon propagator and J^{μ} is the ω-emission current. With the ω-emission current (defined below) taken only in Born approximation, the above transition amplitude corresponds to a distorted-wave Born approximation with no ISI. Equation (1) is diagrammatically depicted in Fig. 1.

Before discussing the structure of J^{μ} in detail let us first specify the NN T matrix. The T matrix used in our calculation is generated by solving a three-dimensional reduced Bethe-Salpeter equation (the Blankenbecler-Sugar equation) for a relativistic one-boson-exchange NN potential V, i.e.,

$$T=V+ViG_{\rm BBS}T \ , \tag{2}$$

where $G_{\rm BBS}$ denotes the Blankenbecler-Sugar (BBS) two-nucleon propagator. In this work we employ the Bonn B NN model as defined in Table A1 of Ref. [18], which includes the π, ρ, ω, σ, η, and a_o mesons. This interaction model fits the NN phase shifts up to the pion threshold energy as well as the NN low-energy parameters and the deuteron properties [18]. It should also be mentioned that each nucleon-nucleon-meson (NNM) vertex in the NN potential is supplemented by a form factor either of monopole or dipole form. We refer to [18] for further details. Furthermore we note that the two-nucleon propagator G_f appearing in Eq. (1) is, for consistency, also chosen to be the BBS propagator, $G_f=G_{f;\rm BBS}$.

The ω-emission current J^{μ} in Eq. (1) is given by the sum of the nucleonic and meson-exchange currents, $J^{\mu}=J^{\mu}_{\rm nuc}+J^{\mu}_{\rm mec}$, as illustrated diagrammatically in Fig. 2. The nucleonic current is defined as

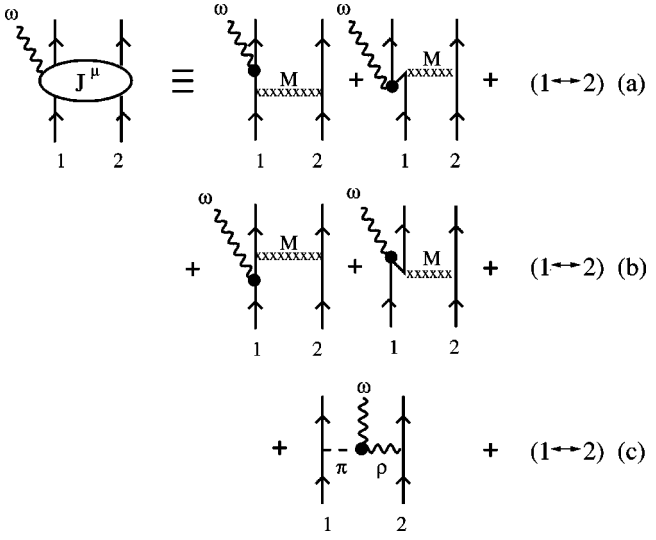

FIG. 2. ω-meson production currents, J^{μ}, included in the present study. (a) and (b) are the nucleonic current, and (c) is the meson exchange current. $M=\pi,\eta,\rho,\omega,\sigma,a_o$.

$$J^{\mu}_{\rm nuc}=\sum_{j=1,2}(\Gamma^{\mu}_j iS_j U+UiS_j\Gamma^{\mu}_j), \tag{3}$$

with Γ^{μ}_j denoting the $NN\omega$ vertex and S_j the nucleon (Feynman) propagator for nucleon j. The summation runs over the two interacting nucleons, 1 and 2. U stands for the meson-exchange NN potential. It is, in principle, identical to the potential V appearing in the NN scattering equation, except that here meson retardation effects [which are neglected in the potential entering in Eq. (2)] are kept as given by the Feynman prescription. Equation (3) is illustrated in Figs. 2(a) and 2(b), where the contributions arising from both the positive- and negative-energy propagations of the intermediate nucleon are shown explicitly. The positive-energy nucleonic current is sometimes referred to as the external current, while the negative-energy current is known as the pair diagram which, together with meson-exchange currents, constitutes what is called the internal current. In a relativistic formulation like the present one, such terminologies seem unnecessary.

The structure of the $NN\omega$ vertex Γ^{μ} (the subscript $j=1,2$ is omitted), required in Eq. (3) for the production, is given by

$$\Gamma^{\mu}(p',p)=-ig_{NN\omega}\Big[F_V(p',p)\gamma^{\mu} -i\frac{\kappa_{\omega}}{2m_N}F_T(p',p)\sigma^{\mu\nu}k_{\nu}\Big] \ , \tag{4}$$

where $g_{NN\omega}$ denotes the vector coupling constant and $\kappa_{\omega}\equiv f_{NN\omega}/g_{NN\omega}$ with $f_{NN\omega}$ being the tensor coupling constant. p and p' denote the incoming and outgoing nucleon four-momentum, respectively, and $k=p-p'$ the four-momentum of the emitted ω meson. The functions $F_V(p',p)$ and $F_T(p',p)$ are form factors which describe the off-shell coupling of ω to the nucleons. They are normalized to unity when the ω and nucleons are on mass shell, i.e., $F_{V,T}[p'^2$

TABLE I. A compilation of $NN\omega$ coupling constants.

$g^2/4\pi$	$f^2/4\pi$	g	f	f/g	Ref.	Method
23.03	0.33	17.01	-2.04	-0.12		naive VDM
24 $\pm$12	$<$1.	17.37			[19]	EM form factors
8.1$\pm$1.5	0.16$\pm$0.45	10.09	1.42	0.14$\pm$0.20	[20]	NN forward d.r.
35.41	0.90	21.094	-3.37	-0.16	[21]	EM form factors
20.	0.0	15.85	0.0	0.0	[22]	NN scattering
34.6$\pm$0.8	0.93	20.86$\pm$0.25	-3.41$\pm$0.24	-0.16$\pm$0.01	[23]	EM form factors
			-2 to 2		[24]	$\omega\pi\pi\pi$ anomaly
11		11.8			[25]	NN scattering

$=m_N^2, p^2=m_N^2, (p'-p)^2=m_\omega^2]=1$. Note that in Fig. 2(a) we have $p'^2=m_N^2$, and in Fig. 2(b), $p^2=m_N^2$. The produced ω is, of course, always on its mass shell.

At present there is a considerable uncertainty in the $NN\omega$ coupling constants. In Table I we have collected different sets of coupling constants from various analyses [19–24]. We see a broad range of values: $g^2_{NN\omega}/4\pi\sim 8$ to 35 for the vector coupling, and $\kappa_\omega\sim -0.16$ to $+0.14$ for the ratio of tensor to vector coupling. For example, in the full Bonn model [22] a value of $g^2_{NN\omega}/4\pi=20$ is required for a best fit to NN data. Clearly this fairly large number must be considered as an effective coupling strength rather than as the intrinsic $NN\omega$ coupling constant. This has been shown in a recent work by Janssen *et al.* [25], where the contribution of the correlated $\pi\rho$ exchange to the NN interaction has been taken into account explicitly. They found that the additional repulsion provided by the correlated $\pi\rho$ exchange allows $g^2_{NN\omega}/4\pi$ to be reduced by about a factor of 2, leading to an ''intrinsic'' $NN\omega$ coupling constant which is more in line with the value one would obtain from the SU(3) symmetry considerations, $g^2_{NN\omega}=9g^2_{NN\rho}$. In the present work, we adopt the vector coupling constant obtained by Janssen *et al.* [25] which is $g^2_{NN\omega}/4\pi=11$. For κ_ω, we consider the range of $\kappa_\omega\sim -0.3$ to $+0.3$.

Additional uncertainties come from the vertex form factors F_V and F_T. Although one has some idea about the nonlocality of the $NN\omega$ vertex from NN scattering, basically nothing is known about its range relevant for the ω-meson production process discussed here. This is because in NN scattering the exchanged ω is off mass shell, whereas in the present case the ω is produced on-mass shell and the nucleons are off their mass shell. The theoretical understanding of these form factors is beyond the scope of the present paper. Therefore, in analogy to what is usually done in NN potential models, we take $F_V=F_T\equiv F_N$ [18] in the present exploratory study. We assume the form factor to be of the form

$$F_N(l^2)=\left(\frac{n\Lambda_N^4}{n\Lambda_N^4+(l^2-m_N^2)^2}\right)^n, \tag{5}$$

where l^2 denotes the four-momentum squared of either the incoming or outgoing off-shell nucleon, p^2 or p'^2. The cutoff parameter Λ_N and n (integer) are treated as free parameters which are adjusted to fit the ω-production data. Note that if $n\to\infty$, $F_N(l^2)$ becomes a Gaussian function. We also introduce the form factor given by Eq. (5) at those NNM vertices [cf. Eq. (3)] appearing next to the ω-production vertex, where the (intermediate) nucleon and the exchanged mesons are off their mass shell. Therefore, the corresponding form factors are given by the product $F_N(l^2)F_M(q_M^2)$, where M stands for each of the exchanged mesons. The form factor $F_M(q_M^2)$ accounts for the off-shellness of the exchanged meson and is taken consistently with the NN potential used for generating the T matrix.

Besides the nucleonic current, one might think of contributions from the isospin-1/2 nucleon resonances (N^*) to the ω-emission current. However, there are no experimental indications of the known N^* resonances decaying into $\omega+p$. These isospin-1/2 and other nucleon resonances can, therefore, contribute to the ω-meson production only via coupled channels. Since in the present work we restrict ourselves to the energy region far below the nucleon resonance threshold in the final state, the coupling to such a channel should not induce any significant effects. In particular, we do not expect any significant modification of the energy dependence of the ω-production cross section due to such a coupling.

For the meson-exchange current, $J^\mu_{\rm mec}$, we consider the contribution from the $\pi\rho\omega$ vertex which gives rise to the dominant meson-exchange current [Fig. 2(c)]. The $\pi\rho\omega$ vertex required for constructing the meson-exchange current is derived from the Lagrangian density

$$\mathcal{L}_{\pi\rho\omega}=\frac{g_{\pi\rho\omega}}{m_\omega}\varepsilon_{\alpha\beta\nu\mu}\partial^\alpha\vec{\rho}^\beta(x)\cdot\partial^\nu\vec{\pi}(x)\omega^\mu(x)\ , \tag{6}$$

where $\varepsilon_{\alpha\beta\nu\mu}$ denotes the Levi-Civita antisymmetric tensor with $\varepsilon_{0123}=-1$. The exchange current is then given by

$$J^\mu_{\rm mec}=[\Gamma^\alpha_{NN\rho}(q_\rho)]_1 iD_{\alpha\beta}(q_\rho)\Gamma^{\beta\mu}_{\rho\pi\omega}(q_\rho,q_\pi,k_\omega)i\Delta(q_\pi) \times[\Gamma_{NN\pi}(q_\pi)]_2+(1\leftrightarrow 2)\ , \tag{7}$$

where $D_{\alpha\beta}(q_\rho)$ and $\Delta(q_\pi)$ stand for the ρ- and π-meson (Feynman) propagators, respectively. The vertices Γ involved are self-explanatory.

The coupling constant $g_{\pi\rho\omega}$ can be estimated from the decay of the ω meson into π^o and γ in conjunction with vector-meson dominance. According to Ref. [26] $g_{\pi\rho\omega}=10$ at vanishing four-momentum square of the ρ meson. The sign of $g_{\pi\rho\omega}$, which determines the relative sign between the nucleonic and meson-exchange currents, can be inferred, for example, from the analysis of pion photo-production off the nucleon in the 1 GeV region [27].

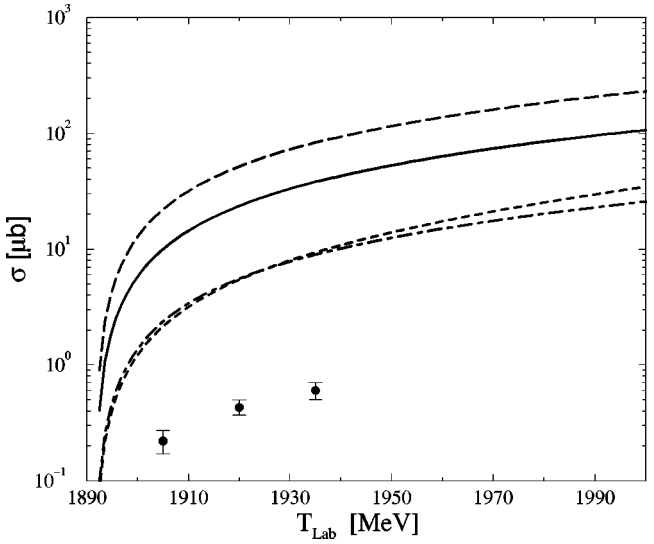

FIG. 3. Total cross section for the reaction $p+p\rightarrow p+p+\omega$ as a function of incident energy. The theoretical results shown here were obtained without including form factors at the ω-production vertices. The short-dashed line is the contribution of the positive-energy nucleonic current alone, the long-dashed line is the contribution of the total (positive + negative) nucleonic current, and the dash-dotted line is the contribution of the meson exchange current. The solid line is the coherent sum of all the contributions. The experimental data are from Ref. [8].

Each vertex in Eq. (7) is accompanied by a form factor. For the $NN\pi$ vertex we use a monopole form factor $F_\pi(q_\pi^2)=(\Lambda_\pi^2-m_\pi^2)/(\Lambda_\pi^2-q_\pi^2)$ with $\Lambda_\pi=1000$ MeV. Note that the cutoff parameter Λ_π required in meson-exchange models of the NN interaction is usually larger than what we use here (e.g., $\Lambda_\pi=1700$ MeV in the NN model applied in the present paper). However, as has been also shown in the previously mentioned work of Janssen *et al.* [25], the $NN\pi$ vertex parameters used in conventional meson-exchange models must be likewise considered as effective values, parametrizing, among other effects, (missing) contributions from the correlated $\pi\rho$ exchange. Indeed, once these contributions are taken into account explicitly (cf. Ref. [25]) the cutoff parameter of the $NN\pi$ vertex goes down to about $\Lambda_\pi=1000$ MeV which is closer to the value of $\Lambda_\pi\sim 800$ MeV obtained from other sources [28–30]. For the $NN\rho$ vertex, we use $F_\rho(q_\rho^2)=[(\Lambda_\rho^2-m_\rho^2)/(\Lambda_\rho^2-q_\rho^2)]^2$ with $\Lambda_\rho=1850$ MeV, consistent with the value in the NN potential [18] that has been used to generate our T matrix. Since nothing is known about the form factor at the $\pi\rho\omega$ vertex where both the π and ρ meson are off their mass shell, we assume the form

$$F_{\pi\rho\omega}(q_\pi^2,q_\rho^2)=F_\pi(q_\pi^2)\left(\frac{\Lambda_\rho^2}{\Lambda_\rho^2-q_\rho^2}\right)^2 \tag{8}$$

with $F_\pi(q_\pi^2)$ given above and $\Lambda_\rho=1850$ MeV. It is normalized to unity at $q_\pi^2=m_\pi^2$ and $q_\rho^2=0$ consistent with the kinematics at which the value of the coupling constant $g_{\pi\rho\omega}=10$ was determined. Quite recently, Friman and Soyeur [31] have used the interaction Lagrangian given by Eq. (6) in conjunction with the vector-dominance model and a form factor of the form $\Lambda_\rho^2/(\Lambda_\rho^2-q_\rho^2)$ with $\Lambda_\rho=m_\rho$ at the $\pi\rho\omega$ vertex in order to fit the Dalitz decay of the ω meson into π^o and $\mu^+\mu^-$. Although this is in a quite different kinematic regime from that involved in the present meson production reaction, we see that our choice of the $\pi\rho\omega$ form factor given by Eq. (8) would lead to an equivalent monopole form factor with $\Lambda_\rho\sim 1300$ MeV when the pion is on its mass shell.

There are, in principle, other meson-exchange currents that could contribute to the ω-meson production in pp collisions. One such potential candidate is due to the $\eta\omega\omega$ vertex which can be obtained from a Lagrangian analogous to that of Eq. (6). The corresponding coupling constant can be estimated from the decay width of ω into η and γ assuming vector dominance. This yields $g_{\eta\omega\omega}\cong 7$, which is comparable to the $\pi\rho\omega$ coupling constant $g_{\pi\rho\omega}\cong 10$. However, the meson-exchange current due to the $\eta\omega\omega$ vertex is about two orders of magnitude smaller than the one involving the $\pi\rho\omega$ vertex, the main reason being the smallness of the $NN\eta$ and $NN\omega$ (tensor) couplings compared to the $NN\pi$ and $NN\rho$ couplings, respectively. The η-meson propagator reduces the cross section only by a factor of 2 compared to the pion propagator. Another exchange current may be due to the $\sigma\omega\omega$ vertex, whose coupling constant may be estimated from the decay width of ω into γ and $\pi^+\pi^-$ or $\pi^0\pi^0$. Assuming an interaction Lagrangian analogous to that given by Eq. (6), we find $g_{\sigma\omega\omega}\sim 0.5$, which is extremely small.

The ω-emission current defined above is, in part, just the Born term of a more general current which can be obtained by using the T-matrix amplitude for the $M+p\rightarrow\omega+p$ transition, where M denotes any meson of interest. In fact, if we disregard the nucleon labeled 2 in Fig. 2 the current becomes nothing else than the Born term of the $M+p\rightarrow\omega+p$ transition amplitude. Figure 2(a), then, would correspond to the s-channel process referred to as the direct pole term, while Fig. 2(b) would correspond to the u-channel process referred to as the exchange (or cross) pole term. Figure 2(c) would correspond to the pion-exchange t-channel process. The T-matrix amplitude for the $M+p\rightarrow\omega+p$ process may be separated into the so-called pole and nonpole terms á la Pearce and Afnan [32]. The pole term is defined just as the (Born) direct pole term mentioned above with the physical nucleon mass and physical $NN\omega$ and NNM vertices. The nonpole term is, then, the difference between the full T matrix and its pole term. Since in the nucleonic current given by Eq. (3) we use the physical nucleon mass and physical $NN\omega$ and NNM vertices, the pole term of the T-matrix amplitude is fully accounted for in the present work. What is taken in the Born approximation is, therefore, the nonpole part of the T matrix only.

III. RESULTS

Once all the ingredients are specified, the total cross section for the reaction $p+p\rightarrow p+p+\omega$ can be calculated. Let us first consider the case where no form factors are used at the ω production vertices [see Eqs. (4),(7)]. We found that the effect of the tensor coupling is essentially to change the absolute magnitude of the cross section without affecting its shape as a function of incident energy in the energy domain considered in this work. The value of $\kappa_\omega=-0.3$ yields the

largest cross section in the range considered for κ_ω, and that the choice of $\kappa_\omega=+0.3$ would lead to a reduction of the cross section by about a factor of 2. In what follows, we assume $\kappa_\omega=-0.3$. The corresponding results are shown in Fig. 3 as a function of the incident proton laboratory energy, together with preliminary data of the SPES3 Collaboration at Saclay [8]. We see that the contributions from the nucleonic (long-dashed line) as well as the mesonic (dash-dotted line) current are much larger than the experimental results. Although these contributions interfere destructively, the total result (solid line) still overestimates the data by nearly two orders of magnitude. Note that in Ref. [8] both the original data and the data shifted in energy (based on a fit to the phase-space energy dependence) have been presented. We show here only the nominal data as the disagreement of the nominal data with the phase-space behavior in Ref. [8] can be due to dynamical effects calculated explicitly in the present paper.

Let us take a closer look at the contribution from the nucleonic current. In the following, we refer to the parts of the nucleonic current arising from the positive-(negative-) energy nucleon propagation in Eq. (3) as the positive-(negative-) energy nucleonic current. As can be seen from Fig. 3, the large nucleonic current contribution (long-dashed line) is dominantly due to the negative-energy component. The positive-energy nucleonic current contribution (short-dashed line) is relatively small. This is opposite to what is known from the $p+p\to p+p+\gamma$ $(pp\gamma)$ reaction. There, both the negative-energy nucleonic and meson-exchange currents are higher-order corrections to the dominant positive-energy nucleonic current [33]. The role of the positive- and negative-energy nucleonic currents can be most easily understood if we consider the ω production at the threshold. We focus on the contribution from the pre-emission diagrams [Fig. 2(b)] which dominate over the post-emission diagrams [Fig. 2(a)] at threshold. The transition amplitude given by Eq. (1) may then be expressed as

$$M\equiv\langle\vec{p}\,',S'M_S'|\epsilon^{*\mu}M_\mu|\vec{p},SM_S\rangle\sim\left(\frac{m_N}{\varepsilon(\vec{p})}\right)\sum_{S''M_S''}\left\{\frac{\langle\vec{p}\,',S'M_S'|T^+|\vec{p},S''M_S''\rangle\langle S''M_S''|\epsilon^{*\mu}\Gamma_\mu^+|SM_S\rangle}{-m_\omega}\right.$$
$$\left.+\frac{\langle\vec{p}\,',S'M_S'|T^-|\vec{p},S''M_S''\rangle\langle S''M_S''|\epsilon^{*\mu}\Gamma_\mu^-|SM_S\rangle}{2\varepsilon(\vec{p})-m_\omega}\right\}\ , \tag{9}$$

where $\vec{p}$ $(\vec{p}\,')$ denotes the initial (final) relative momentum of the two interacting nucleons, S (S') and M_S (M_S') stand for the inital (final) total spin and its projection. ϵ^μ denotes the polarization vector of the emitted ω meson. Here, the superscript $(+/-)$ in T and Γ_μ denotes terms involving a positive- or negative-energy nucleon. $\varepsilon(\vec{p})=\sqrt{\vec{p}^{\ 2}+m_N^2}$, and $\vec{p}\,'=0$ at threshold. In the above equation, $\Gamma_\mu^\pm\equiv\Gamma_{1\mu}^\pm+\Gamma_{2\mu}^\pm$, cf. Eq. (3). Its matrix elements are given by

$$\langle S''M_S''|\epsilon^{*\mu}\Gamma_\mu^+|SM_S\rangle=g_{NN\omega}\frac{\kappa_\omega}{4m_N}\left(\frac{m_\omega}{m_N}\right)|\vec{p}|\ \ [1-(-)^{S''-S}]\langle S''M_S''|\vec{\sigma}_1\cdot(\hat{p}\times\vec{\epsilon})|SM_S\rangle\ \ , \tag{10}$$

with $\hat{p}=\vec{p}/|\vec{p}|$, and

$$\langle S''M_S''|\epsilon^{*\mu}\Gamma_\mu^-|SM_S\rangle=ig_{NN\omega}[1+(-)^{S''-S}]$$
$$\times\left\{\left(1-\kappa_\omega\frac{m_\omega}{2m_N}\right)\left(\frac{\varepsilon(\vec{p})-m_N}{m_N}\right)\vec{\epsilon}\cdot\hat{p}\langle S''M_S''|\vec{\sigma}_1\cdot\hat{p}|SM_S\rangle-\left(\frac{\varepsilon(\vec{p})}{m_N}+\kappa_\omega\frac{m_\omega}{2m_N}\right)\langle S''M_S''|\vec{\sigma}_1\cdot\vec{\epsilon}|SM_S\rangle\right\}. \tag{11}$$

The first term in Eq. (9) corresponds to the positive-energy and the second term to the negative-energy nucleonic current contribution. It is obvious that, due to the nonzero mass of the ω meson, the ratio between the negative- and positive-energy nucleonic current contributions is much larger compared to the $pp\gamma$ reaction. This is simply a consequence of the fact that the intermediate nucleon is far off-shell at least by an amount of the mass of the emitted ω meson. In the $pp\gamma$ reaction, the positive-energy contribution leads to the well-known infrared divergence due to the massless nature of the emitted photon. In the present case, a further enhancement of the negative-energy contribution relative to the one from the positive-energy current arises from the smallness of the tensor-to-vector coupling ratio, κ_ω, as can easily be seen by comparing Eqs. (10) and (11).

It is also interesting to note that the positive-energy nucleonic current contribution at threshold involves only the tensor coupling $f_{NN\omega}=g_{NN\omega}\kappa_\omega$ [cf. Eq. (10)]. This can be understood as follows: in the limit of small momentum of the emitted ω meson, i.e., $\vec{k}\to0$, the matrix element of the $NN\omega$ vertex for the jth nucleon is given by

$$\langle\overline{u(\vec{p})}|\epsilon_\mu^*\Gamma_j^\mu|u(\vec{p})\rangle=-i\vec{\epsilon}\cdot[g_{NN\omega}(\vec{p}_j/m_N)+i(f_{NN\omega}/4m_N)$$
$$\times(m_\omega/m_N)(\vec{\sigma}_j\times\vec{p}_j)]. \tag{12}$$

At threshold, the Pauli principle requires the two protons to be in a relative $^1S_0$ final state which, together with the ω meson having total $J^P=1^-$, implies that the initial two protons are in a $^3P_1$ state. To get a nonvanishing contribution the production operator therefore has to change the total spin of the NN subsystem which is possible only with the tensor coupling and not with the vector coupling as can be seen from the expression for the ω-production vertex given by Eq. (12). Actually, the feature that the positive-energy nucleonic current contribution is independent of the vector coupling, $g_{NN\omega}$, holds not only at threshold but also at any incident energy, provided the momentum of the emitted ω meson goes to zero. This is because in this limit the vector coupling leads only to the convection current for positive-energy nucleon propagation [first term in Eq. (12)] and the total convection current should vanish for identical particles in their center-of-mass frame.

In principle, there are two ways for bringing the theoretical results in agreement with the experimental data. One is simply to readjust the relevant coupling constants in order to obtain a more complete cancellation between the nucleonic and mesonic currents. The other possibility is to introduce form factors at the ω-production vertices, as discussed in Sec. II. The first alternative would require a rather drastic change of the coupling constants, beyond the uncertainties discussed in the previous section. Therefore, in the present analysis we choose the second alternative. The introduction of form factors within our model is also well motivated because the ω-meson production reaction is a highly off-shell process. Indeed, in both the nucleonic and meson-exchange current diagrams shown in Figs. 2(a)–2(c) all the intermediate particles are highly off their mass shell. Specifically, for an incident energy corresponding to the ω-production threshold, the intermediate nucleon in Fig. 2(a) is off its mass shell by $p^2-m_N^2\sim 2.3$ GeV^2 and the nucleon in Fig. 2(b) is $p^2-m_N^2\sim -1.5$ GeV^2 off-shell. Similarly, for the π and ρ mesons in Fig. 2(c) we have $q_\pi^2-m_\pi^2\sim -0.8$ GeV^2 and $q_\rho^2-m_\rho^2\sim -1.4$ GeV^2.

Results including the form factors [Eqs. (5),(8)] at the ω production vertices [Eqs. (4),(7)] are shown in Fig. 4. With our choice for the $\pi\rho\omega$ vertex [cf. the discussion after Eq. (8)] the cutoff mass Λ_N is the only free parameter to be adjusted to the data. [The parameter n in Eq. (5) has been fixed to be $n=1$.] Since the meson-exchange current contribution alone already exceeds the data (cf. dash-dotted line in Fig. 4) and due to the destructive interference between the nucleonic and mesonic currents we can find two solutions, one with the nucleonic current contribution being larger than the mesonic current contribution, and another one with the nucleonic current being smaller than the mesonic current contribution. The long-dashed line is the nucleonic current contribution corresponding to $\Lambda_N=1160$ MeV in Eq. (5) which yields the total contribution given by the dotted line ($NC>MEC$) when it is added coherently to the mesonic current (dash-dotted curve). The short-dashed line is the nucleonic current contribution corresponding to $\Lambda_N=850$ MeV which leads to the total contribution given by the solid line ($NC<MEC$). We see that the energy dependence of the two solutions are different. Since the form factors necessarily introduce an energy dependence, we have checked whether

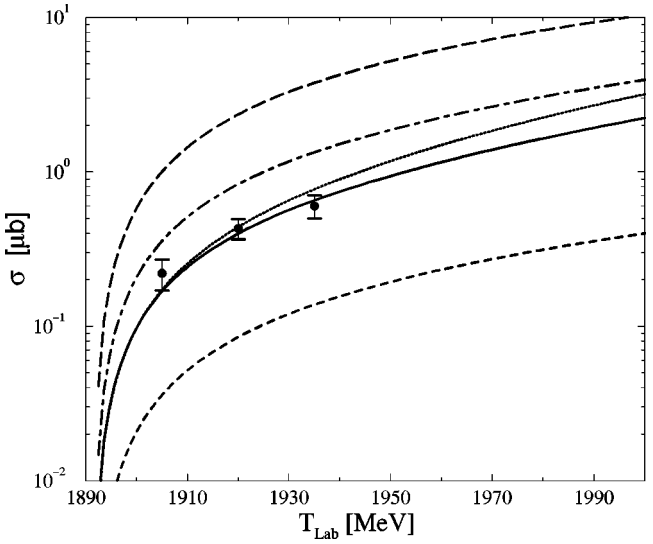

FIG. 4. Total cross section for the reaction $p+p\rightarrow p+p+\omega$ as a function of incident energy. The theoretical results shown here include form factors as described in Sec. II. The dash-dotted line is the contribution of the meson exchange current. The long-dashed (short-dashed) line is the contribution of the nucleonic current based on the cutoff mass Λ_N = 1160 (850) MeV [cf. Eq. (5)]. The coherent sum of the two contributions where the nucleonic current is larger than the mesonic current (Λ_N = 1160 MeV) is given by the dotted line, the one where the nucleonic current is smaller than the mesonic current (Λ_N = 850 MeV) is given by the full line. The experimental data are from Ref. [8].

this difference in the energy dependence between the two solutions is just an artifact of the particular form of the form factor [Eq. (5)] used in the present work. To this end, we employed different types of form factors at the $NN\omega$ vertex, such as a Gaussian form. We found that the feature exhibited by the two solutions in Fig. 4 persists.

In order to demonstrate the difference in the energy dependence our results are shown again in Fig. 5 over a larger

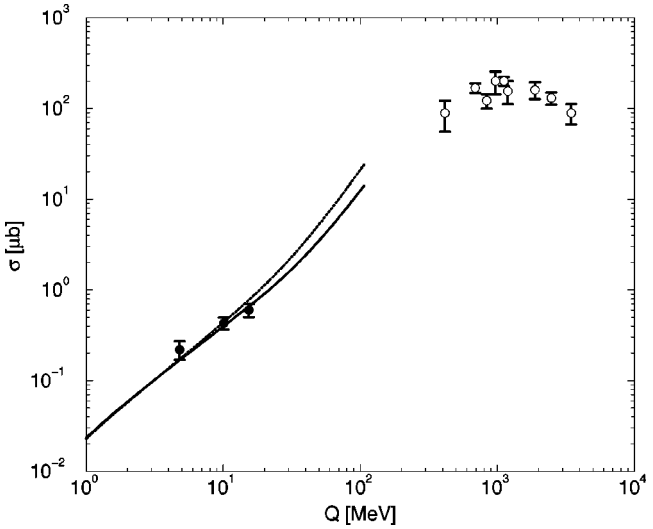

FIG. 5. Total cross section for the reaction $p+p\rightarrow p+p+\omega$ as a function of the excess energy $Q=\sqrt{s}-\sqrt{s_o}$. The curves are the same as in Fig. 4 extended up to $T_{\rm lab}=2.2$ GeV. The high-energy data are taken from Ref. [34].

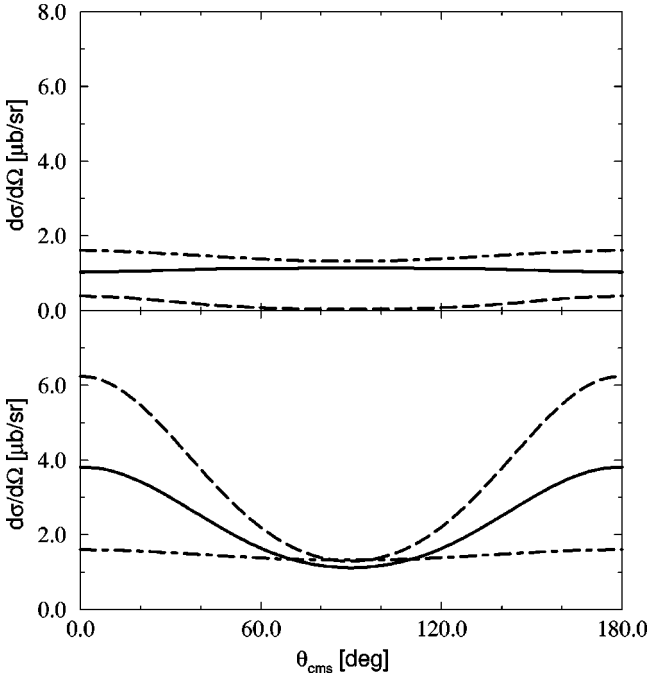

FIG. 6. Angular distribution of the emitted ω mesons in the total c.m. system at the energy $T_{\rm lab}=2.2$ GeV. The lower figure shows the result where the nucleonic current is larger than the mesonic current ($NC>MEC$) whereas the upper graph contains the results where the nucleonic current is smaller than the mesonic current ($NC<MEC$). The dash-dotted line is the contribution of the mesonic current, the long-dashed line is the contribution of the nucleonic current and the full line is the total result.

energy range and as a function of excess energy, $Q\equiv\sqrt{s}-\sqrt{s_o}$, where $\sqrt{s}$ denotes the total energy of the system and $\sqrt{s_o}=2m_N+m_\omega$, its ω-production threshold energy. Here we also display the experimental data from Ref. [34] at higher energies. Our model calculations are carried out up to the energy at which the FSI becomes inelastic, which corresponds to an incident energy of around $T_{\rm lab}=2.2$ GeV. Already in this energy range one observes a difference in the predicted cross sections for the two scenarios ($NC\lessgtr MEC$) considered. Therefore, in principle, measurements of the cross section for $Q\sim 100$ MeV and higher could be useful in determining the relative magnitude of the two production mechanisms.

In Fig. 6 we present angular distributions of the emitted ω mesons in the total center-of-mass (c.m.) system at an incident energy of $T_{\rm lab}=2.2$ GeV for the two scenarios discussed above ($NC\lessgtr MEC$). As can be seen, the two scenarios lead to dramatically different angular distributions: strong anisotropy in the case of nucleonic current contribution being larger than the mesonic current contribution ($NC>MEC$, lower figure) and an almost isotropic distribution in the case of nucleonic current being smaller than the mesonic current contribution ($NC<MEC$, upper figure). The strong anisotropy of the $\cos^2\theta$ shape introduced by the nucleonic current is due to the spin-dependent part of the current, sometimes referred to as the magnetization current [35]. To leading order, its contribution to the differential cross section is given by

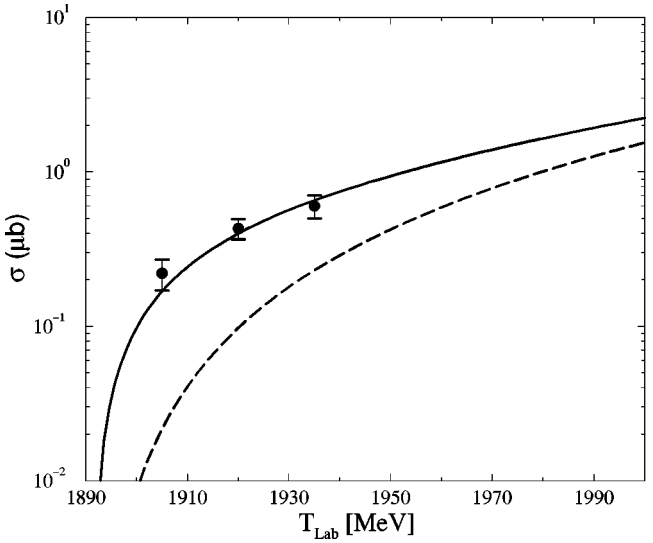

FIG. 7. The effect of the final-state interaction on the total ω-production cross section. The full and dashed lines correspond to the results with and without final-state interaction, respectively. These results correspond to the choice of the nucleonic current being larger than the mesonic current ($NC>MEC$).

$$\frac{d^2\sigma_{\rm magn}}{dWd\Omega}\cong(a^2+b^2v'^2)+c^2v^2\cos^2(\theta)\ , \qquad (13)$$

where v (v') denotes the relative velocity of the two interacting nucleons in the initial (final) state. a, b, and c are smooth functions of the energy W of the emitted ω meson and of the total energy of the system. It should be clear from Fig. 6 that the angular distribution provides an unique and clear signal for discriminating between the two considered ω-production scenarios. We also note that if the mesonic current contribution were larger than the present prediction, we would have a much more pronounced angular dependence for the case of $NC<MEC$ than that shown in Fig. 4. Indeed, the angular distribution would exhibit a peak around $\theta=90°$, where it shows a valley in the case of $NC>MEC$. We emphasize that the shape of the angular distribution is determined by the magnitude of each contribution. Therefore, by measuring the angular distribution one should be able to extract uniquely the magnitude of the individual contributions.

The effect of the FSI is extremely important in any particle production process where the interacting nucleons are left in a low-energy s-wave state. This is demonstrated in Fig. 7 where the results with and without FSI are shown. Close to the threshold the FSI enhances the total cross section by almost an order of magnitude. No FSI effects were taken into account in recent calculations [10,11]. In view of this, in our opinion, the rather good agreement of the peripheral on-shell rescattering model [10] must be considered as rather accidental.

IV. SUMMARY

We have investigated the $p+p\to p+p+\omega$ reaction within a relativistic meson-exchange model. It has been found that the nucleonic and $\pi\rho\omega$ exchange currents are the two potential sources contributing to the ω production in this

reaction, and that they interfere destructively. The calculation ignoring the nonlocalities of the ω-production vertices leads to a dramatic overestimation of preliminary SPES3 data [8]. We interpret this as a manifestation of off-shell effects in hadronic vertices within our model. In the absence of a microscopic prescription, we introduce phenomenological form factors to account for the off-shell effects in the vertex functions and fix the free parameters by fitting to the SPES3 data. It is, then, found that the positive-energy nucleonic current contribution is very small compared to the negative-energy nucleonic and the $\pi\rho\omega$ meson-exchange current contribution.

We find that the relative magnitude of the contributions from the nucleonic current and the meson-exchange currents influences the energy dependence of the predicted $p+p \rightarrow p+p+\omega$ cross section. Therefore, from a measurement of the cross sections as a function of incident energy one should, in principle, be able to identify the dominant reaction mechanism for ω production. As our most important result, we find that the angular distribution of the emitted ω meson depends sensitively on the strength of the individual contributions. A study of the angular distribution should therefore allow one to determine uniquely the magnitude of each contribution. A measurement of this observable, which can be carried out at modern accerelators, would be of great importance for understanding ω production in NN collisions.

ACKNOWLEDGMENTS

We are indebted to Wolfgang Kühn for a discussion of experiments being carried out at SATURNE and to Collin Wilkin and Francois Hibou for exchange of information concerning the SPES3 experiment [8]. We also thank Gary Love for a careful reading of the manuscript. This work was partially supported by the DLR grant, project No. POL-81-94.

[1] A. Shor, Phys. Rev. Lett. **54**, 1122 (1985).
[2] G.E. Brown and M. Rho, Phys. Rev. Lett. **66**, 2720 (1991).
[3] T. Hatsuda and S.H. Lee, Phys. Rev. C **46**, R34 (1992).
[4] M. Asakawa and C.M. Ko, Nucl. Phys. **A560**, 399 (1993); Phys. Rev. C **48**, R526 (1993).
[5] R. Wurzinger *et al.*, Phys. Rev. C **51**, R443 (1995).
[6] G. Fäldt and C. Wilkin, Phys. Lett. B **354**, 20 (1995).
[7] L.A. Kondratyuk and Y.N. Uzikov, JETP Lett. **63**, 1 (1996).
[8] Collaboration CRN Strasbourg, IPN Orsay, LNS Saclay, in *Nouvelles de Saturne no. 19*, p. 51 (Saclay, 1995).
[9] S. Brauksiepe *et al.*, Nucl. Instrum. Methods Phys. Res. A **376**, 397 (1996).
[10] A.A. Sibirtsev, Nucl. Phys. **A604**, 455 (1996).
[11] W.S. Chung, G.Q. Li, and C.M. Ko, Phys. Lett. B **401**, 1 (1997).
[12] Y.S. Golubeva, A.S. Iljinov, and I.A. Pshenichnov, Nucl. Phys. **A562**, 389 (1993).
[13] A. Sibirtsev, W. Cassing, and U. Mosel, Z. Phys. A **358**, 357 (1997).
[14] W.S. Chung, G.Q. Li, and C.M. Ko, Phys. Lett. B **401**, 1 (1997); Nucl. Phys. **A625**, 347 (1997).
[15] K. Nakayama, Phys. Rev. C **39**, 1475 (1989).
[16] H.O. Meyer *et al.*, Phys. Rev. Lett. **65**, 2846 (1990).
[17] M. Batinić, A. Švarc, and T.-S.H. Lee, Phys. Scr. **56**, 321 (1997).
[18] R. Machleidt, Adv. Nucl. Phys. **19**, 189 (1989).
[19] G. Höhler, E. Pietarinen, I. Sabba-Stefanescu, F. Borkowski, G.G. Simon, V.H. Walther and R.D. Wendling, Nucl. Phys. **B114**, 505 (1976).
[20] W. Grein and P. Kroll, Nucl. Phys. **A338**, 332 (1980).
[21] S. Furuichi and K. Watanabe, Prog. Theor. Phys. **82**, 581 (1989); **83**, 565 (1990).
[22] R. Machleidt, K. Holinde, and Ch. Elster, Phys. Rep. **149**, 1 (1987).
[23] P. Mergell, U.G. Meissner, and D. Drechsel, Nucl. Phys. **A596**, 367 (1996).
[24] J. Speth and R. Tegen, Z. Phys. C **75**, 717 (1997).
[25] G. Janssen, K. Holinde, and J. Speth, Phys. Rev. C **54**, 2218 (1995).
[26] J.W. Durso, Phys. Lett. B **184**, 348 (1987).
[27] H. Garcilazo and E. Moya de Guerra, Nucl. Phys. **A562**, 521 (1993).
[28] S.A. Coon and M.D. Scadron, Phys. Rev. C **23**, 1150 (1981); **πN** Newslett. **3**, 90 (1991).
[29] A.W. Thomas and K. Holinde, Phys. Rev. Lett. **63**, 2025 (1989).
[30] K.F. Liu, S.J. Dong, T. Draper, and W. Wilcox, Phys. Rev. Lett. **74**, 2172 (1995).
[31] B. Friman and M. Soyeur, Nucl. Phys. **A600**, 477 (1996).
[32] B. C. Pearce and I. R. Afnan, Phys. Rev. C **34**, 991 (1986).
[33] F. de Jong and K. Nakayama, Phys. Rev. C **52**, 2377 (1995); Phys. Lett. B **385**, 33 (1996).
[34] V. Flaminio *et al.*, CERN preprint CERN-HERA 84-01 (1984); R. Baldi *et al.*, Phys. Lett. **68B**, 381 (1977).
[35] V. Herrmann, J. Speth, and K. Nakayama, Phys. Rev. C **43**, 394 (1991).